Hydrogen Atom Transfer as a Key Step in Base Metal Catalysis

Sudha Yadav

(MS15029)

A dissertation submitted for the partial fulfillment

of BS-MS dual degree in Science.

Indian Institute of Science Education and Research Mohali

April 2020

Certificate of Examination

This is to certify that the dissertation titled "Hydrogen Atom Transfer as a Key Step in Base Metal Catalysis" submitted by Ms Sudha Yadav (Reg. No. MS15029) for the partial fulfillment of BS-MS dual degree programme of the Institute, has been examined by the thesis committee duly appointed by the Institute. The committee finds the work done by the candidate satisfactory and recommends that the report be accepted.

Dr. Angshuman Roy Choudhury Dr. Ujjal K. Gautam Dr. Debashis Adhikari
(Supervisor)

Declaration

The work presented in this dissertation has been carried out by me under the guidance of Dr. Debashis Adhikari at the Indian Institute of Science Education and Research Mohali. This work has not been submitted in part or in full for a degree, a diploma, or a fellowship to any other university or institute. Whenever contributions of others are involved, every effort is made to indicate this clearly, with due acknowledgement of collaborative research and discussions. This thesis is a bonafide record of original work done by me and all sources listed within have been detailed in the bibliography.

Sudha Yadav

In my capacity as the supervisor of the candidate's project work, I certify that the above statements by the candidate are true to the best of my knowledge.

Dr. Debashis Adhikari
(Supervisor)

Acknowledgement

I would like to dedicate this thesis to my parents for supporting me throughout these five years of my undergraduate studies. My sincere thanks to my superheroes Sudhanshu and Himanshu for being a wonderful companion.

My sincere thanks to the Department of Science and Technology, Government of India for the INSPIRE fellowship of five years. My heartfelt gratitude to IISER Mohali for providing a highly intellectually stimulating and competitive environment for my undergraduate studies.

I would like to sincerely thank my thesis supervisor Dr. Debashis Adhikari for being a huge moral support and constant motivation throughout this one year of my master's thesis. My special thanks to him for believing in my capability and giving me immense confidence that kept me enthusiastic throughout the year. I would also like to express my gratitude to my committee members Dr. Angshuman Roy Choudhary and Dr. Ujjal K. Gautam for their useful suggestions and encouragement.

I would like to thank Amreen K. Bains for her continuous support, for teaching me all important laboratory techniques and for being the most amazing person giving me all the affection and care. I would also like to thank Abhishek Kundu for this invaluable support and confidence in me this entire year. It was a nice experience to work in such a good atmosphere created by DA Lab group members.

My sincere thanks to Sandita, Amit, Ahina, Subhankar, and Poonam for being an emotional support throughout these five years. I owe a lot of memories to all of them.

Sudha Yadav

List of Figures

List of Tables

List of Schemes

List of Notations

aq.	Aqueous
Ar	Aryl
Bu	Butyl
d	Doublet
DCM	Dichloromethane
dd	Doublet Of Doublet
eq.	Equation
equiv.	Equivalent
HOMO	Highest Occupied Molecular Orbital
iPr	Isopropyl
IR	Infrared Region
KO^tBu	Potassium tert-butoxide
m	Mutiplet
Me	Methyl
MeCN	Acetonitrile
mg	Milligram
ml	Millilitres
mL	Millilitre
mmol	Millimole
NMR	Nuclear Magnetic Resonance
o	Degree
Ph	Phenyl
Ppm	Parts Per Million

rt	Room temperature
UV	Ultra-Violet
Vis	Visible
μL	micro-litre

Contents

Abstract

The major theme of the work presented in this dissertation is to develop an understanding of hydrogen atom transfer (HAT) and investigate it thoroughly. An inexpensive and green nickel catalyst does a wide range of catalysis including N-alkylation and formation of benzazoles starting from alcohol and amines. In case of N-alkylation, the reduced backbone of nickel catalyst extracts hydrogens during the alcohol oxidation process, stores it and redelivers it to imine in order to form amine. The alcohol oxidation step has been studied elaborately. The establishment of HAT is done by a series of experiments, as kinetic studies, KIE measurements, Kreevoy's criteria, Evans Polanyi plot and intermediate isolation. In the other part of thesis, the formation of benzazoles is discussed. A reaction sequence for the formation of benzazoles is alcohol oxidation, imine formation, ring cyclization and dehydrogenative aromatization. Both the alcohol oxidation and amine dehydrogenation steps are directly mediated by HAT, at fairly mild reaction conditions. By doing kinetic and KIE measurements, HAT is well established here too.

Chapter 1

Hydrogen Atom Transfer As a Key Step in Base Metal Catalysis - N-alkylation

1.1 Introduction

Base Metal Catalysis

Catalysis is a powerful method that is now widely used in the industry for the transformation of organic molecules into lucrative products. A catalyzed reaction has multiple benefits over an uncatalyzed one that includes regio and stereoselectivity.[1,2]

Metals like Platinum (Pt), Palladium (Pd), Rhodium (Rh), Ruthenium (Ru) have been used in catalysis for decades and are often at the frontiers of a new breakthrough in catalysis. These metals can perform the $2e^-$ redox processes, which are typically favored during organometallic catalysis. Major reactions performed by these metals are hydroboration[3], arylation[4], amination[5], hydrosilylation[6] etc. The main drawback of using these metals in the industry is their high cost and limited availability.

Base metal catalysis has seen exponential growth in recent times. Notably in the reactions like hydroboration[7], arylation[8], amination[9], which were limited to precious metals. Main group elements[10] and organocatalysts[11] have emerged as "greener" alternatives for such reactions. Metal-ligand cooperativity has played an important role in enabling first row transition metal catalysis of reactions that undergo two-electron

processes. The right combination of first-row transition metals with different types of ligands can catalyze reaction efficiently and effectively that were limited to precious metals only.

Redox active or Non-innocent ligands

When we can assign metal oxidation state without any difficulty from redox activity of the ligands, we call those ligands as "innocent" ligands. One classic example of a complex having such ligand is Werner complex $[Co(NH_3)_4Cl_2]Cl$. It's a Co^{III} compound as ligands are redox inactive clearly. On the other hand, ligands for which such an oxidation state ambiguity is possible were considered noninnocent in Jorgensen's definition.[9] With a redox active ligand, the ligand can be the dominant electron source or sink, with the metal retaining its original oxidation state.

For example, if a spin-paired complex schematically represented as M–L is reduced by $1e^-$, the product might be better represented either as $M^{\bullet -}$–L if the ligand is redox inactive, or as $M–L^{\bullet -}$ if not. In reality, M and L will both be affected by the reduction and the resulting unpaired electron density will be shared over both.

Redox active ligands form part of the broader group of multifunctional ligands[10] a group that has attracted increasing interest, in catalytic applications. These ligands are capable to communicate novel reactivity to the adjacent metal complexes by modulating the loss or gain of electrons and protons thus allowing the framework to adopt different resonance structures and consequently provide new ligand properties. The substrate involved in the catalysis can also be poised to bind to a molecular recognition unit to impart regio- and stereospecificity to the desired catalytic transformation.[11,12]

Hydrogen atom transfer

Hydrogen atom transfer involves the transfer of a proton and an electron. From the most basic process combustion to enzymatic catalysis, HAT is the most rudimentary step.[13]

$$A-H + B \rightarrow A + H-B$$

Recently, metalloenzyme active sites have been shown to oxidize substrates by HAT, which has open a way to explore the transition metal mediated HAT.

Classical organic HAT reactions have an abstracting group that is a p-block radical $X^{\bullet}$. In contrast, transition metal complexes that abstract $H^{\bullet}$ typically have an oxidizing metal center to accept the electron and a basic ligand to accept the proton.[14] These are sometimes known as proton-coupled electron transfer (PCET) reactions because of the possible separation of the e^- and H^+.[15]

HAT activates R-H bonds in a very particular way, like the way a reaction occurs can be changed by changing suitable hydrogen abstractor, solvent conditions, temperature etc. Evans Polanyi provides us with a correlation between rate constants and bond dissociation energies to determine whether HAT is a rate-limiting step or not. There are various theoretical and experimental methods present for the determination of HAT like Marcus theory, KIE determination, free energy calculations etc.

1.2 EXPERIMENTAL SECTION

General Information

1.2.1 Chemicals

All the reagents and solvents used for synthesis were laboratory grade purchased from AVRA chemicals, Sigma Aldrich and TCI chemicals and were used without further purification. Solvents such as methanol, ethanol and toluene were used as received from the suppliers. The reaction progress during synthesis was monitored by thin layer chromatography (Sigma Aldrich) and visualized under UV light (254 nm). Column chromatography was performed using SD Fine silica gel 60-120 mesh using a gradient of ethyl acetate and hexane as mobile phase.

1.2.2 Spectroscopic Measurements

^{1}H NMR and ^{13}C NMR spectra were recorded on a 400 MHz Bruker Biospin Advance III FT-NMR spectrometer. The solvent used for measurement is $CDCl_3$ for all the products. UV-Vis Spectroscopic measurements were recorded on PerkinElmer LAMBDA 365 UV/Visa-NIR spectrophotometer using a 1mm path length quartz cuvette at room temperature. High-resolution mass spectra were recorded on a Waters QTOF mass spectrometer. GC-MS was recorded on Agilent 7890B GC coupled to 5977B GC/MSD with HP-5MS column. Standard analysis software was used for analysis and visualization of the spectra. Python was used for fitting the curves and all plots were plotted using Origin 2018.

1.2.3 Synthesis

1.2.3.1 Preparation of 3,5-di(tert-butyl)-2-hydroxy azobenzene (L) :

To an aqueous solution of 0.01 mmol of aniline, 0.04 mmol of Conc. HCl was added until the solution was clear. The mixture was cooled below 0 ^{o}C. After that a solution of 0.011 mmol of solution nitrile was added dropwise. An ethanolic solution of 0.01 mmol 2, 4-Di-*tert*-butylphenol was added to the preformed diazonium solution made in the previous step. Upon addition of the phenol, color of the solution changed to red instantaneously. Then, the solution was filtered to obtain 3,5-di(tert-butyl)-2-hydroxy azobenzene (**L**) as a red-brownish solid. A single spot in the TLC suggested the reaction was complete with no impurities.

1.2.3.2 Preparation of $Ni(Azo)_2$ (1)* :

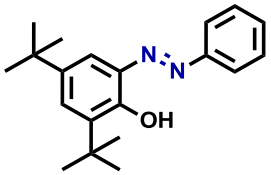

L

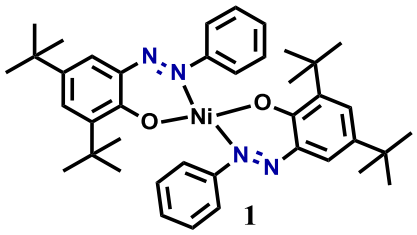

1

A methanolic solution of 0.1 mmol of L was taken in a 100 mL round-bottom flask and to it 0.1 mmol of KOH was added and the mixture was stirred at rt for 30 min. Then, 0.05 mmol of Ni(OAc)2 was added to the reaction mixture and refluxed for 30 min. Immediate precipitate was obtained during the reflux. After completion of the reaction, the solution was filtered to obtain **1** in 82 % yield. Spectroscopically the identity and the purity of the molecule was ensured. (* Synthesis of the complex has been carried out by Amreen K. Bains).[15]

1.2.4 Catalysis

1.2.4.1 N-alkylation of amine by hydrogen borrowing method

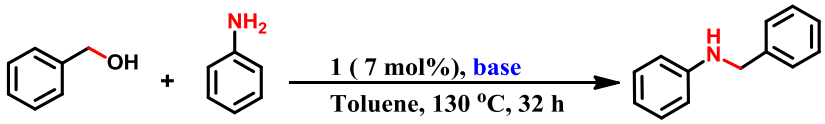

Scheme 1.1. Amination of aromatic alcohols

In a 25 mL oven dried flask, alcohols (1.0 mmol), amines (0.25 mmol), *t*-BuOK (0.25 mmol), **1** (7 mol%) were added followed by 10 mL toluene. Upon charging all chemicals the reaction flask was evacuated and filled with nitrogen. The reaction mixture was heated at 130 ^{o}C for 32 h. The reaction mixture was cooled to room temperature upon completion and concentrated *in vacuo.* The residue was purified by column chromatography using a petroleum ether/ethyl acetate (5-10%) as eluent to afford pure products.

1.2.4.2 Bis-alkylation

In a 25 mL oven dried flask, alcohols (1.0 mmol), amines (0.5 mmol), *t*-BuOK (0.25 mmol), **1** (7 mol%) were added followed by 10 mL toluene. Upon charging all chemicals the reaction flask was evacuated and filled with nitrogen. The reaction mixture was heated at 130 ^{o}C for 32 h. The reaction mixture was cooled to room temperature upon completion and concentrated *in vacuo.* The residue was purified by column chromatography using a petroleum ether/ethyl acetate (5-10%) as eluent to afford pure products.

1.3 Results and Discussion

1.3.1 Azo: Potential redox backbone for N-alkylation

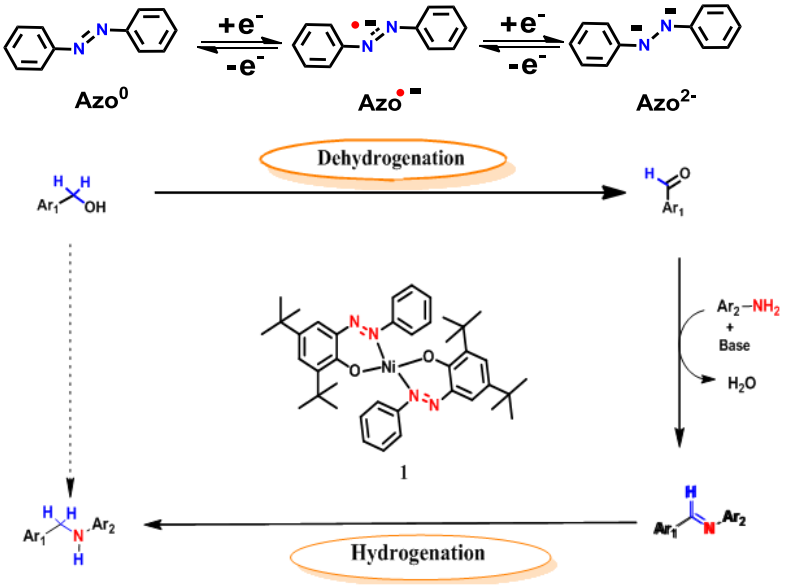

Figure 1.1 Hypothesis of N-alkylation mediated by Hydrogen Atom Transfer

$Ni(azo)_2$ is a well-defined and benchstable azo-phenolate ligand-coordinated nickel catalyst which can efficiently execute N-alkylation of a variety of anilines by alcohol. The redox-active azo ligand can store hydorgen generated during alcohol oxidation and redelivers the same to an in-situ-generated imine bond to result in N-alkylation of amines (Figure 1.1). The reaction has wide scope, and a large array of alcohols can directly couple to a variety of anilines. To understand the dehydrogenation step, a series of experiments was done and hypothesized the plausible mechanism.

1.3.2 Kinetics analysis for alcohol oxidation : with respect to *catalyst loading*

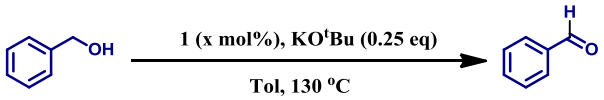

To understand the mechanism of the reaction, we performed detailed kinetic analysis of the reaction. In order to examine the dependence of reaction rate on the catalyst during alcohol oxidation, we studied the rate of benzaldehyde formation as a function of catalyst loading variation. Increasing the concentration of **1** over the range from (x = 2.5 to 10 mol% with respect to benzyl alcohol) displayed a linear increase in the rate, k_{obs} for the oxidation of alcohol.

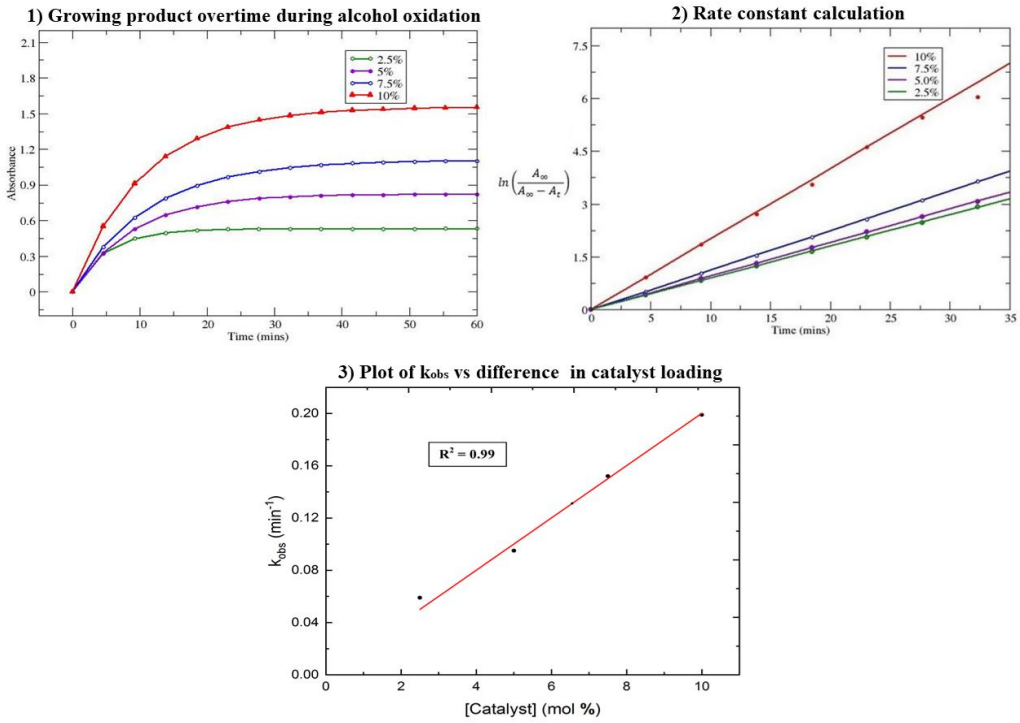

Figure 1.2 Pseudo-First order kinetic analysis for oxidation of benzyl alcohol: with respect to catalyst loading

1.3.3 Kinetics analysis for alcohol oxidation : with respect to *substrate loading*

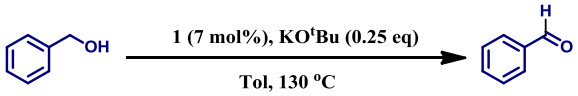

In order to examine the dependence of reaction rate on the substrate during alcohol oxidation, we studied the rate of benzaldehyde formation as a function of substrate loading variation. Increasing the concentration of substrate over the range from (80 time to 140 times with respect to **1**) displayed a linear increse in the rate, k_{obs} for the oxidation of alcohol.

From this set of experiments the rate law for the alcohol dehydrogenation can be derived as rate = k[**1**][benzyl alcohol], which further suggests the substrate remains bound to the catalyst at the rate-determining step.

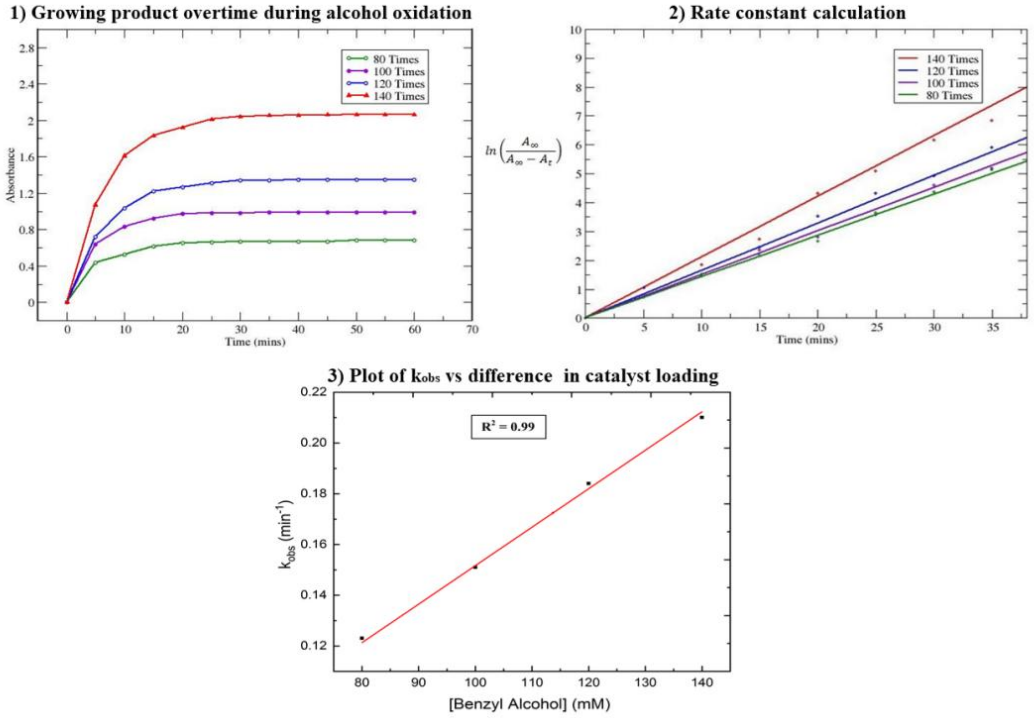

Figure 1.3 Pseudo-First order kinetic analysis for oxidation of benzyl alcohol: with respect to substrate loading

1.3.4 Saturation Kinetics for alcohol oxidation

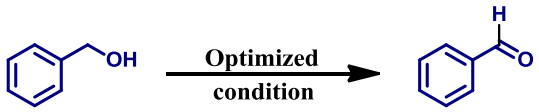

Reaction condition: **1** (5 mol%), benzyl alcohol (1 mmol), KO^{t}Bu (0.25 mmol), toluene (2 mL), 25 ^{o}C, 35 ^{o}C, 45 ^{o}C , 100 min.

To make sure that alcohol truly binds to the nickel center before its oxidation, saturation kinetics experiment with a considerable excess of benzyl alcohol was performed. The saturation curves were obtained when the concentration of the alcohols were exceeding 1.0 M (Figure 1.4). We conducted the saturation kinetics studies at three different temperatures (25–45 ^{o}C, Figure 1.5 and 1.6) and fitted the data according to saturation rate law **(**equation 1**).**[16]

$$[1]^{-} + \text{benzyl alcohol} \overset{K}{\rightleftharpoons} [1.\text{benzyl alcohol}]^{-} \xrightarrow{k} \text{product}$$

$$k_{obs} = \frac{kK[\text{benzyl alcohol}]}{1 + K[\text{benzyl alcohol}]} \quad \cdots(1)$$

From the saturation kinetics data gathered at room temperature, an equilibrium constant was calculated to be 66.68 M^{-1} along with rate constant 0.000105 s^{-1}. A considerable value of the equilibrium constant strongly indicates the binding of the alcohol (likely in the form of an alkoxide) to nickel.

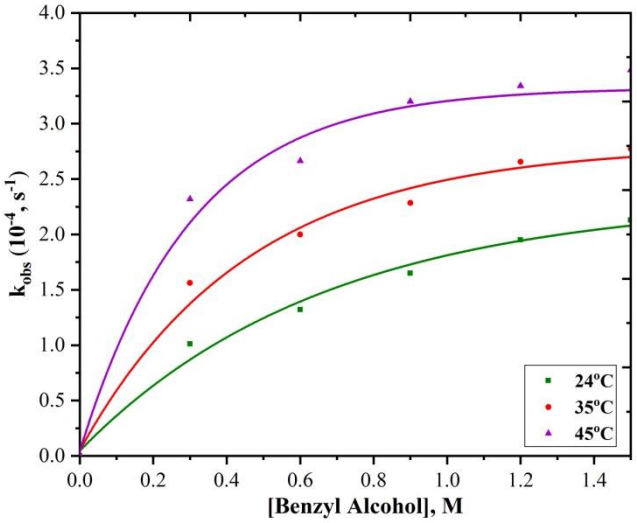

Figure 1.4 Saturation Kinetics of Benzyl alcohol

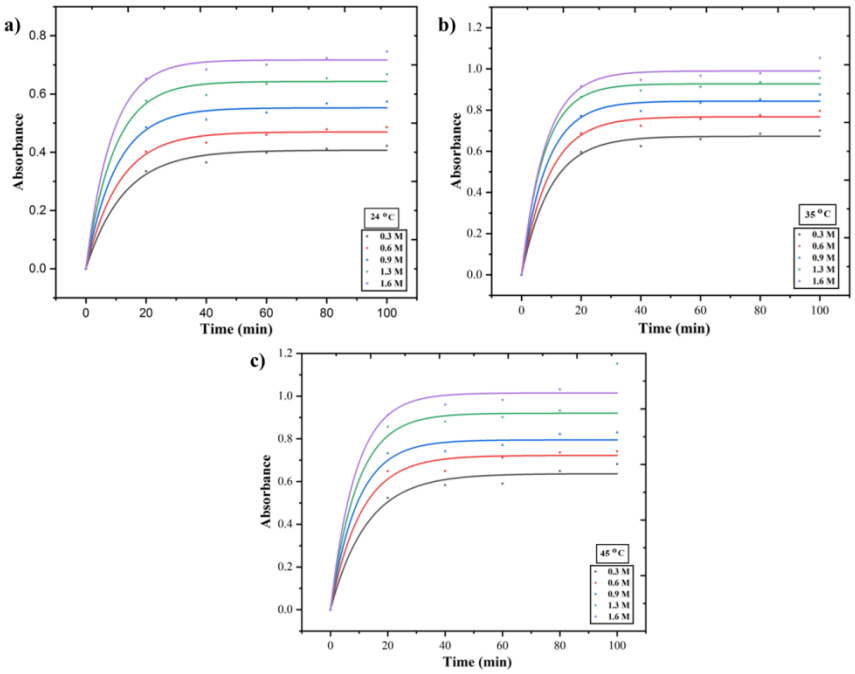

Figure 1.5 Kinetics profile of the alcohol oxidation at a) 24 ^{o}C, b) 35 ^{o}C, c) 45 ^{o}C varying concentration of benzyl alcohol

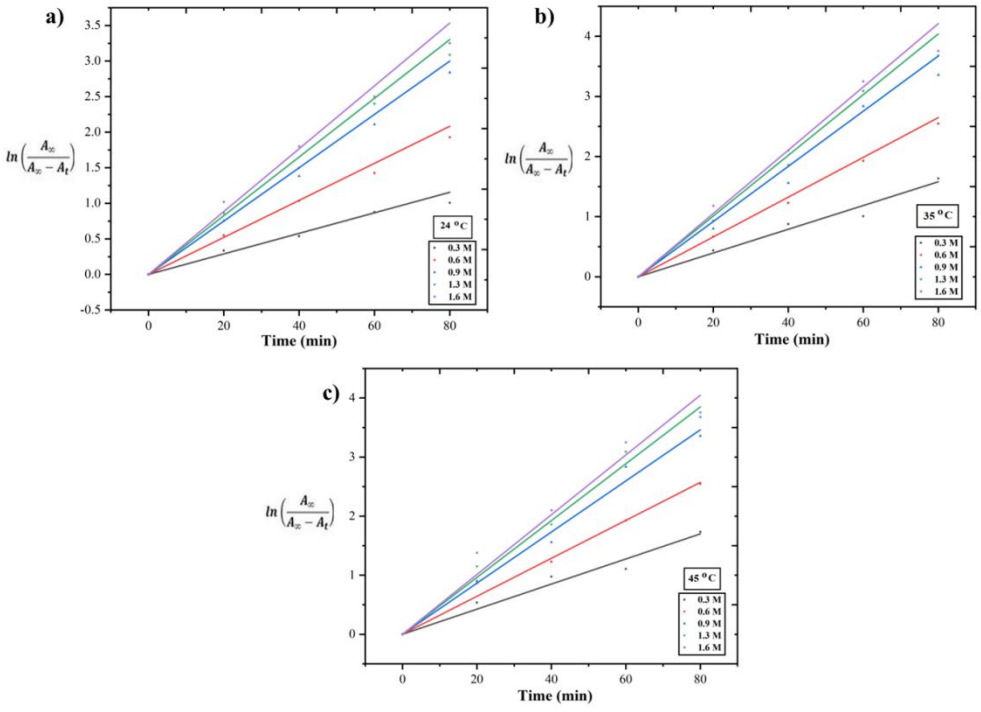

Figure 1.6 Rate constant calculations for saturation kinetics profile of the alcohol oxidation at a) 24 ^{o}C, b) 35 ^{o}C, c) 45 ^{o}C varying concentration of benzyl alcohol

1.3.5 Van't Hoff Plot for alcohol oxidation

The above discussed plots disclosed the corresponding equilibrium and rate constants at the respective temperature (Table 1.1 and 1.2). The experiment was repeated twice to confirm the values.

Set 1:

S.No	Temperature (^{o}C)	K (M^{-1})	k_{obs} (10^{-4} s^{-1})
1.	24	66.68	1.05
2.	35	57.39	1.27
3.	45	49.4	1.37

Table 1.1 Set 1 of Van't Hoff experiment

Set 2:

S.No	Temperature (^{o}C)	K (M^{-1})	k_{obs} (10^{-2} s^{-1})
1.	24	65.1	1.09
2.	35	58.35	1.30
3.	45	50.1	1.39

Table 1.2 Set 2 of Van't Hoff experiment

As expected, with increasing temperature the value of the equilibrium constant consistently decreases while the magnitude of rate constant increases. We plotted the logarithm of K vs 1/T to extract the thermodynamic parameters for the binding. Interestingly, ΔH of -2.5 ± 0.50 kcal mol^{-1} and the ΔS of -1.13 cal mol^{-1} K^{-1} were the calculated values from van't Hoff plot (Figure 1.7). The enthalpy change is very small and detachment of the phenolate arm upon protonation by the bound alcohol likely compensates the new Ni-alkoxide bond formation.

$$\text{Van't hoff Equation:} \quad \mathbf{ln(K)} = \frac{-\Delta \mathbf{H}}{\mathbf{RT}} + \frac{\Delta \mathbf{S}}{\mathbf{R}}$$

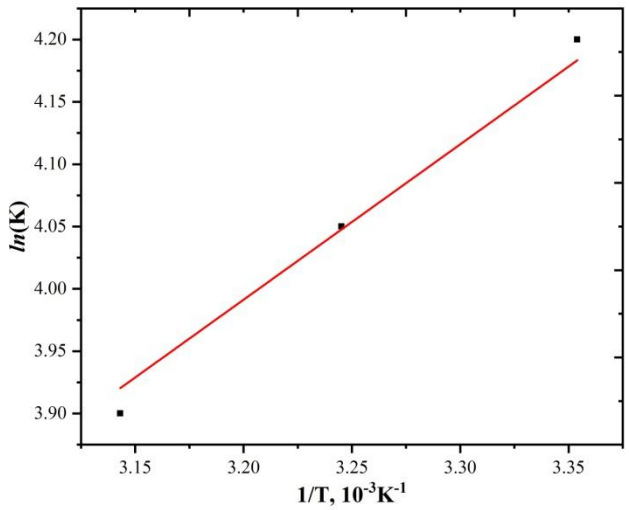

Figure 1.7 Van't Hoff plot for Alcohol Oxidation

1.3.6 Eyring Analysis

The temperature-dependent kinetic experiments were performed to know the barrier for HAT reaction. The Eyring plot disclosed a $\Delta H^{\ddagger}$ of 20.31 ± 1.57 kcal mol^{-1} while the $\Delta S^{\ddagger}$ to be -18.59 ± 1.11 cal mol^{-1} K^{-1} (Figure 1.8). The negative $\Delta S^{\ddagger}$ value corroborates with the bimolecular nature of the rate-limiting step. The overall reaction barrier, $\Delta G^{\ddagger}$ of 25.85 ± 3.61 kcal mol^{-1} for the process asserts that the alcohol oxidation component of the reaction can proceed at room temperature, which is also supported by the experimental facts.

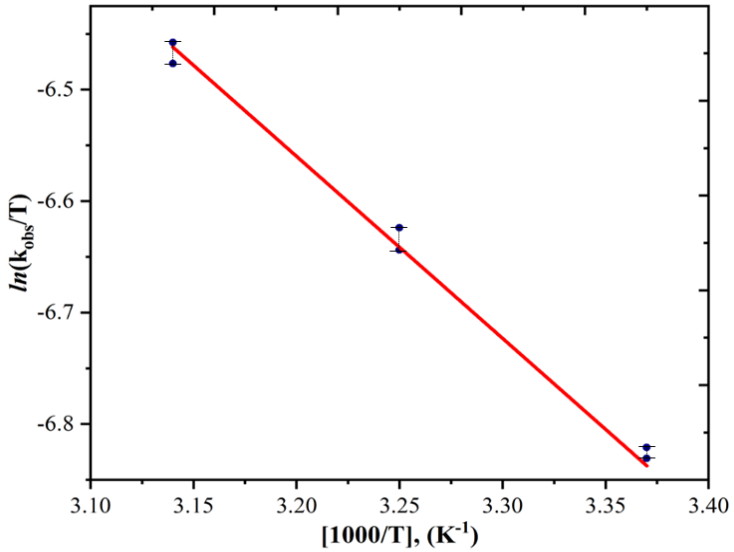

Figure 1.8 Eyring plot for Alcohol Oxidation

1.3.7 Kinetic Isotope Effect for alcohol oxidation

The nickel bound alkoxide transfers a hydrogen atom to the monoreduced azo group to procced for the oxidation. We tried to prove this HAT based alcohol oxidation from detailed kinetic isotope effect (KIE).

From Transition state theory, at room temperature, k_H/k_D was found to be 4.3 at 298 K. Interestingly, the experimentally measured KIE at room temperature (15.6) was far higher than the theoretically projected value stemming from zero point energy (ZPE) difference.

$$k = \frac{k_B T}{h} e^{-\left(\frac{\Delta G^{\ddagger}}{RT}\right)} \qquad \frac{k_H}{k_D} = e^{-\left(\frac{\Delta\Delta G^{\ddagger}}{RT}\right)}$$

The large, nonclassical KIE value indicates azo-radical based hydrogen atom abstraction from the α-CH of benzyl alcohol and that C–H bond cleavage is the rate-determining step for the alcohol oxidation step. Notably, this system provides an excellent opportunity to investigate the HAT from a carbon to nitrogen radical as a function of temperature. The high value of KIE implicates that that rate of HAT is considerably contributed by quantum mechanical tunneling. To investigate the HAT step further, the -KIE was measured at three other temperatures.

1.3.7.1 Kinetic studies of benzyl alcohol

In a 5 mL vial, 1.0 mmol $PhCH_2OH$, 0.25 mmol KO^tBu and 5 mol% of **1** were added followed by 2 mL of toluene. This reaction mixture was heated at 10, 24, 35, 45 °C for 100 min (Figure 1.9).

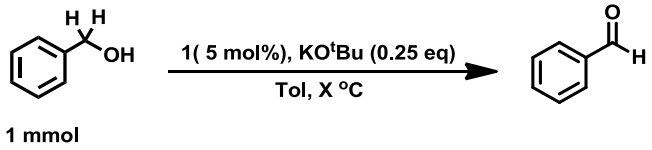

1.3.7.2 Kinetic Studies of deuterated benzyl alcohol

In a 5 mL vial, 1.0 mmol $PhCD_2OH$, 0.25 mmol KO^tBu and 5 mol% of **1** and were added followed by 2 mL of toluene. This reaction mixture was heated at 10, 24, 35, 45 °C for 100 min (Figure 1.10).

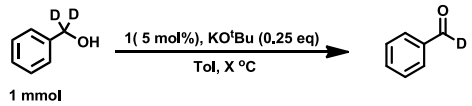

1.3.7.3 Rate constant calculation for benzyl alcohol and deuterated benzyl alcohol

Data obtained from UV-Vis and GC in above experiments was fitted in first order equation and corresponding rate constants were calculated. Rate constants for both, benzyl alcohol and deuterated benzyl alcohol, were plotted in single graph to observe a clear comparison at each temperature (Figure 1.11) and KIE was calculated.

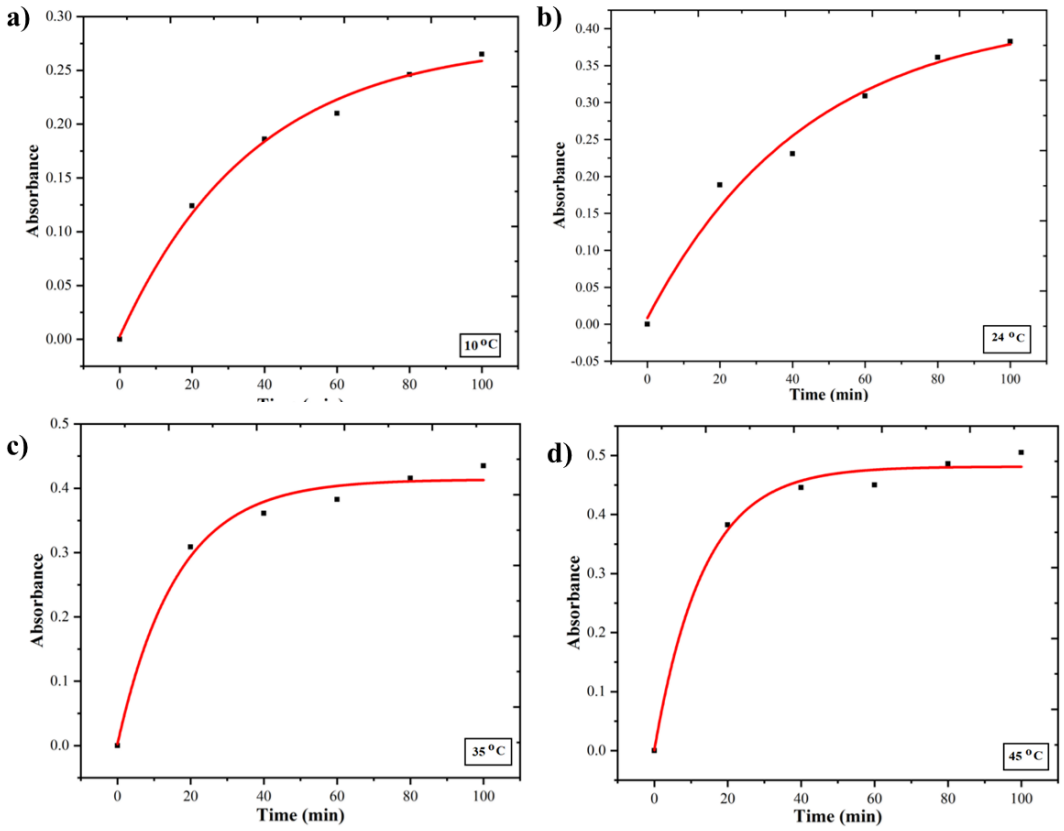

Figure 1.9 Product formation plot (traced via UV-Vis spectroscopy) from $PhCH_2OH$ at a) 10 °C, b) 24 °C, c) 35 °C, d) 45 °C.

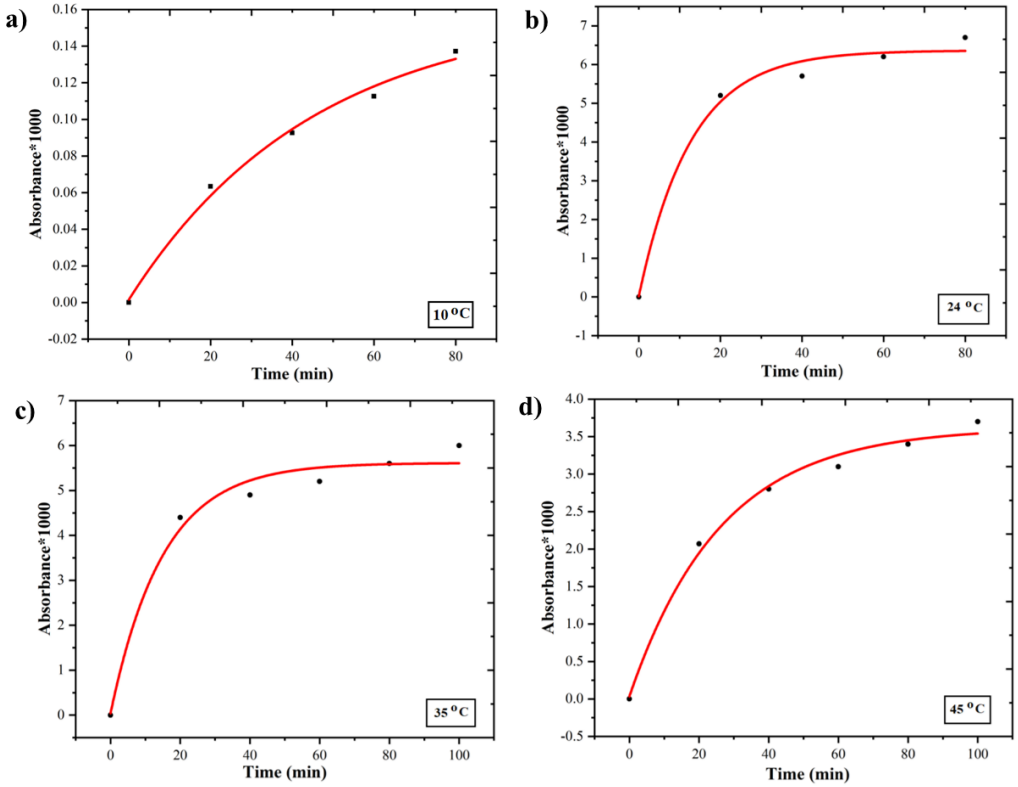

Figure 1.10 Product formation plot (traced via UV-Vis spectroscopy) for $PhCD_2OH$ at a) 10 °C, b) 24 °C, c) 35 °C, d) 45 °C

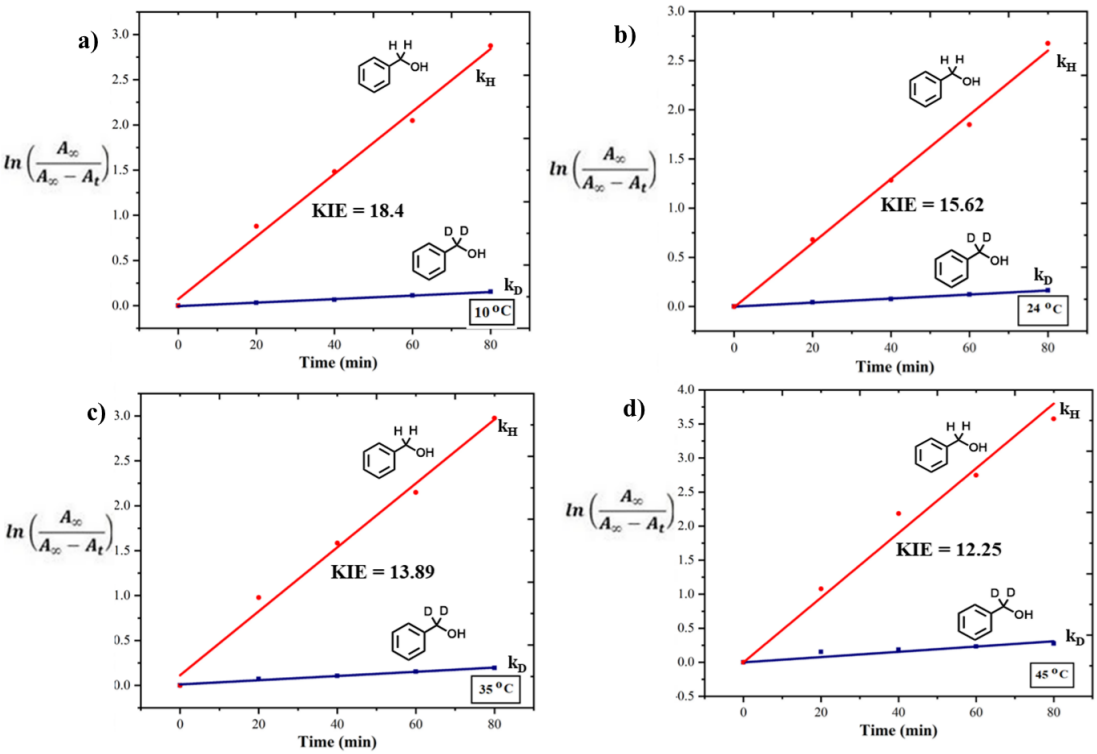

Figure 1.11 KIE for alcohol oxidation measured at a) 10 °C, b) 24 °C, c) 35 °C, d) 45 °C

1.3.8 Arrhenius plot for alcohol oxidation

After measuring KIE at different temperatures (Table 1.3), we plotted it in Arrhenius fashion, ln(KIE) over 1/T. The plot clearly exhibits inverse temperature dependence of isotope effect and a nice correlation as a straight line whose slope and intercept describes the A_H/A_D and $E_{aD}–E_{aH}$ respectively. For the HAT step involved in alcohol oxidation, these A_H/A_D and $E_{aD}–E_{aH}$ values were observed to be 0.47 and 2.05 kcal mol^{-1} (Figure 1.12). All these values regarding KIE measurements strongly indicate for nonclassical hydrogen tunneling in accord with Kreevoy's criteria of the tunneling contribution to the HAT step.

S.No	Temperature (^oC)	KIE (k_H/k_D)
1.	10	18.40
2.	24	15.62
3.	35	13.89
4.	45	12.25

Table 1.3 KIE values at all temperatures for alcohol oxidation

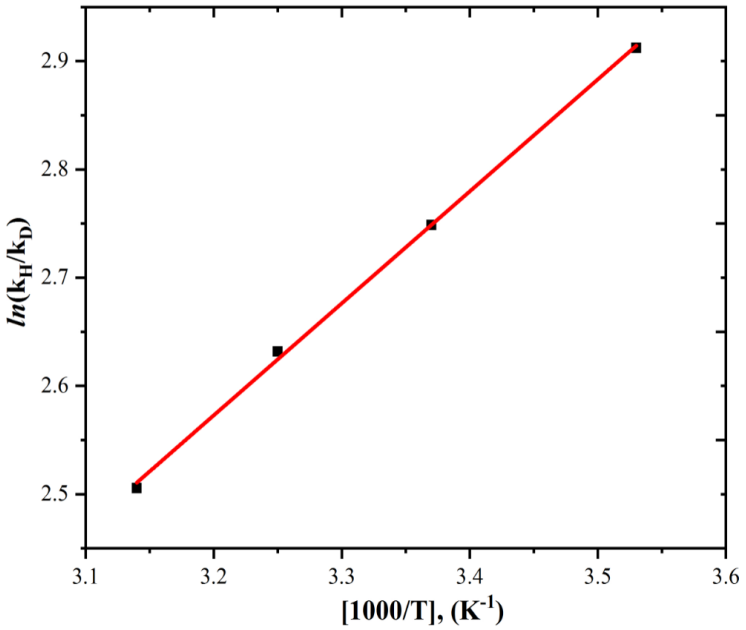

Figure 1.12 Arrhenius plot

1.3.9 Evans-Polanyi type correlation

We found a Evans-Polanyi type correlation of reaction rate and bond dissociation free-energy for a set of five alcohols whose C–H bond strength varies over ~15 kcal mol^{-1} (Figure 1.13). As suggested by Mayer, this pattern also implicates the presence of HAT as a rate determining step.[17]

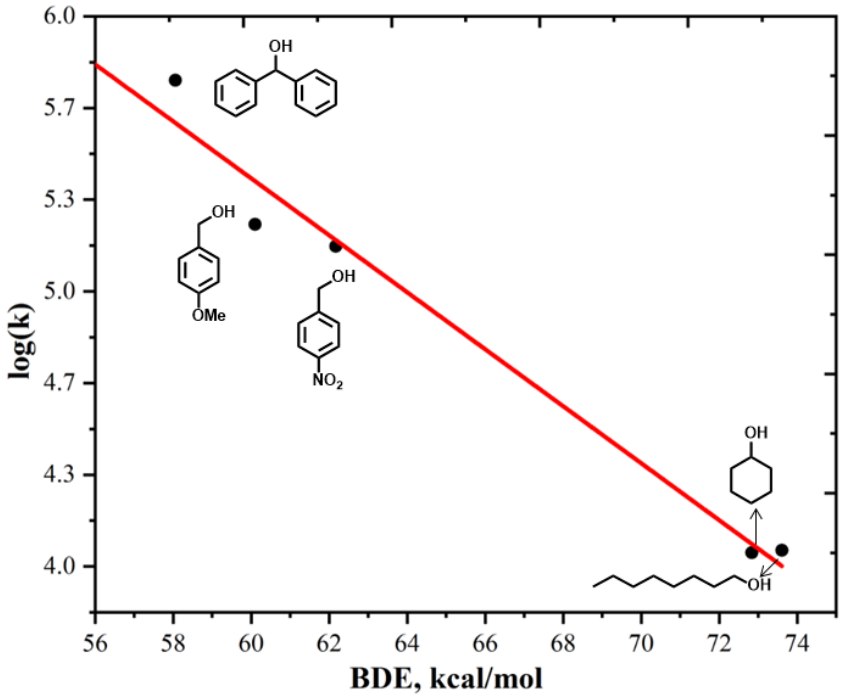

Figure 1.13 Linear free energy correlation

1.3.10 Hammett plot for alcohol oxidation catalyzed by 1

Consistent with the radical process and subsequent ketyl radical generation via HAT during alcohol oxidation, *para*- substitution of the benzyl alcohol did not influence the rate of HAT (Figure 1.14). Plotting the rate of HAT for multiple benzyl alcohol substrates with electron donating and withdrawing groups at the *para*-position as a function of σ_p^+ values provided a very small ρ value of 0.05. Such a minor dependence on rate was also documented earlier for GOase model (ρ = -0.14).[18] The lack of any influence of electron-withdrawing and -donating groups on the reaction rate strongly suggests that the HAT is present here.

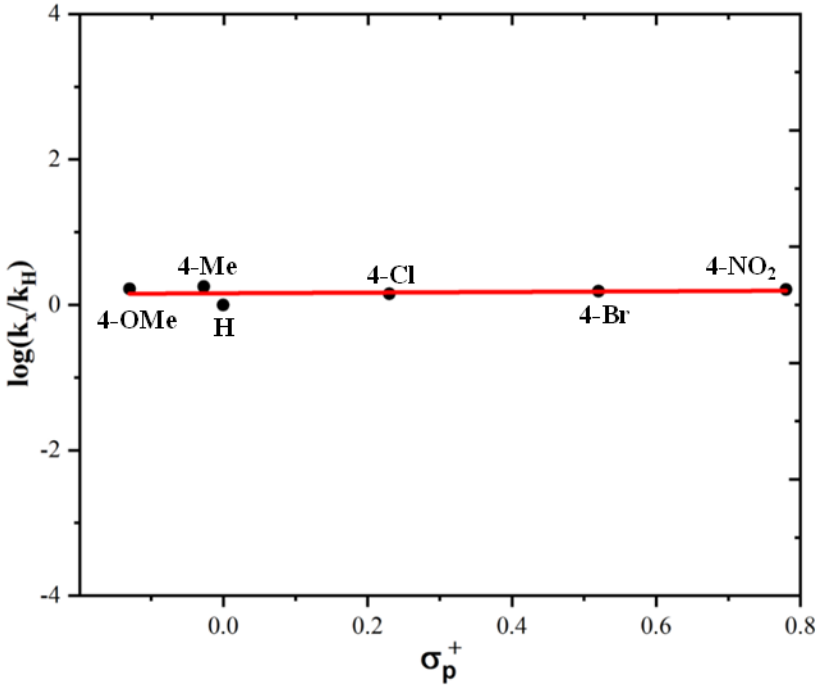

Figure 1.14 Hammett plot

1.4 Summary

In this chapter, we presented a homogeneous, single-site catalyst comprising of a redox-active azo ligand and base metal nickel which efficiently performs N-alkylation of a variety of amines starting from alcohol. A broad scope of substrates has been shown for N-alkylation, which proves the versatile nature of the catalyst.

The ligand chosen for such base metal catalyst is instrumental, given its direct participation in the alcohol oxidation step via HAT. HAT is established using a series of experiments starting from kinetic studies, Evans Polanyi correlation, kinetic isotope effect determination etc.

A large kinetic isotope effect (KIE, 15.6 at 24 ^{o}C) has been recorded during alcohol oxidation, suggesting significant non-classical tunneling contribution to HAT. Indeed, the A_H/A_D and $E_{aD}–E_{aH}$ were observed experimentally as 0.47 and 2.05 kcal mol^{-1} from Arrhenius plot of KIE, which ensures quantum mechanical tunneling using Kreevoy's Criteria. Consistent with the radical process and subsequent ketyl radical generation via HAT during alcohol oxidation, *para*- substitution of the benzyl alcohol did not influence the rate of HAT. To prove that, a thorough hammett analysis has been done. From all the experiments discussed above, we have a thorough understanding of plausible mechanism and isolated all the targeted intermediates.

Chapter 2

Investigating HAT mediated base metal catalysis in Benzazoles

2.1 Introduction

Dehydrogenation reactions

Dehydrogenation, in general, concerns the abstraction of hydrogen from a compound to produce a less saturated analog. Dehydrogenation reactions are of major industrial importance, especially in the production of constituents for the manufacture of high-octane gasoline. The alcohol dehydrogenation reactions have captured attention recently, as the process can provide a very inexpensive source of alkyl groups.[19] The dehydrogenation of low boiling alkanes has become of great industrial importance because it presents an alternative method for obtaining alkenes. Utilizing this highly abundant and cheap source of alkyls, multiple synthetic methodologies have been discovered lately to assemble value-added heterocyclic rings.[20]

Benimidazoles

Benzimidazole derivative are associated with various types of pharmaceutical products. Benzimidazole nucleus is one of the bioactive heterocyclic compounds that exhibit a range of biological activities. Specifically, this nucleus is a constituent of vitamin B12. First synthesis of benzimidazole formation via dehydrogenative coupling was showcased by Watanabe which required noble metal catalyst ruthenium at a very high temperature, 215 ^{o}C.[21] Recent examples from Kempe involve Ir-based catalysts which synthesize benzimidazoles and substituted benzimidazoles. Some heterogeneous systems have also been developed for the synthesis of benzimidazoles but those comprise of precious metals Ir and Ru.[22]

On the contrary, base metal representatives for this important transformation are only handful although, cobalt, nickel and manganese catalysts started appearing promising in dehydrogenative coupling of diamine and alcohols to realize benzimidazole derivatives.[23] A major drawback of these systems are the requirement of relatively harsh reaction conditions and long reaction time. Additionally, rational design of catalysts is challenging because of the lack of precise mechanistic understanding.

2.2 EXPERIMENTAL SECTION

2.2.1 Chemicals

Specifications same as mentioned in section 1.2.1

2.2.2 Synthesis

2.2.2.1 General procedure for synthesis of benzimidazole: variety of benzyl alcohol, aliphatic alcohols and substituted diamines

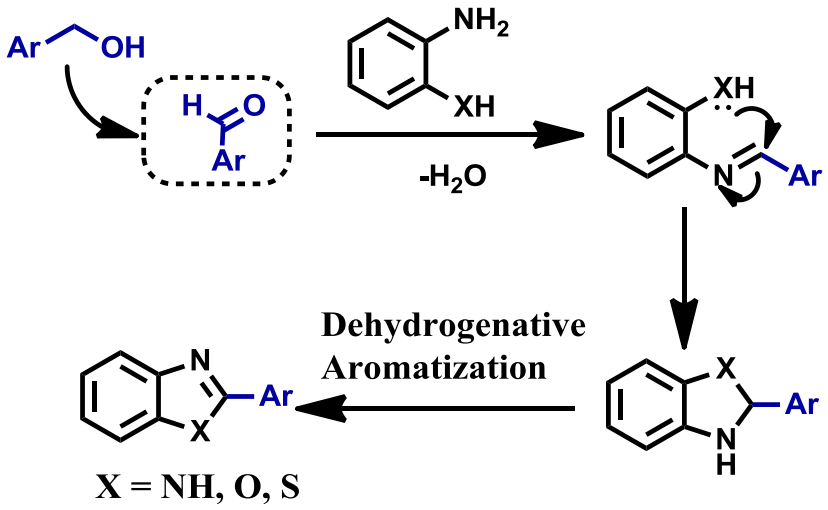

Scheme 2.1 Route to benzazoles

In a typical reaction 5 mL vial was charged with alcohols (1 mmol), *o*-phenylenediamine (1 mmol), KO^{t}Bu (0.5 mmol), **1** (5 mol%) in 2 mL toluene and was closed with rubber septum. The resulting solution was spurged with O_2. The reaction mixture was stirred at 80 ^oC for 10 h. The reaction mixture was cooled to room temperature upon completion and concentrated *in vacuo.* The residue was purified by column chromatography using petroleum ether/ethyl acetate (5-10%) as eluent to afford pure products. The desired coupling products were fully characterized by ^1H, ^{13}C NMR spectroscopies.

2.2.2.2 General procedure for synthesis of benzimidazole: di-alcohols

In a typical reaction 5 mL vial was charged with alcohols (0.5 mmol), o-phenylenediamine (1 mmol), KO^{t}Bu (0.5 mmol), **1** (5 mol%) in 2 mL toluene and was closed with rubber septum. The resulting solution was spurged with O_2. The reaction mixture was stirred at 80 ^oC for 10 h. The reaction mixture was cooled to room temperature upon completion and concentrated in vacuo. The residue was purified by column chromatography using petroleum ether/ethyl acetate (5-10%) as eluent to afford pure products. The desired coupling products were fully characterized by ^1H, ^{13}C NMR spectroscopies.

2.2.2.3 General procedure for synthesis of 1,2 di-substituted benzimidazole

In a typical reaction 5 mL vial was charged with alcohols (2 mmol), o-phenylenediamine (1 mmol), KO^{t}Bu (0.5 mmol), **1** (5 mol%) in 2 mL toluene and was closed with rubber septum. The resulting solution was spurged with O_2. The reaction mixture was stirred at 80 ^oC for 10 h. The reaction mixture was cooled to room temperature upon completion and concentrated in vacuo. The residue was purified by column chromatography using petroleum ether/ethyl acetate (5-10%) as eluent to afford pure products. The desired coupling products were fully characterized by ^1H, ^{13}C NMR spectroscopies.

2.2.2.4 General procedure for for synthesis of benzthiazole and benzoxazoles

In a typical reaction 5 mL vial was charged with alcohols (1 mmol), 2-aminothiophenol/2-aminophenol (1 mmol), KO^{t}Bu (0.5 mmol), **1** (5 mol%) in 2 mL toluene and was closed with rubber septum. The resulting solution was spurged with O_2. The reaction mixture was stirred at 80 ^oC for 10 h. The reaction mixture was cooled to room temperature upon completion and concentrated in vacuo. The residue was purified by column chromatography using petroleum ether/ethyl acetate (5-10%) as eluent to afford pure products. The desired coupling products were fully characterized by ^1H, ^{13}C NMR spectroscopies.

2.3 Results and Discussions

2.3.1 Optimization of reaction conditions for benzimidazole synthesis *

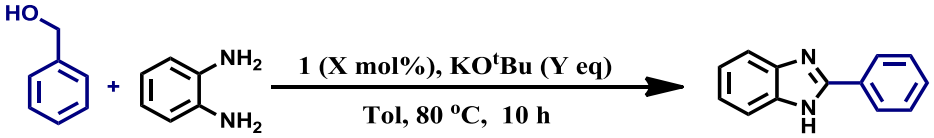

Scheme 2.2 Optimization of Benzimidazole synthesis

Entry	Catalyst	Base	Product (Yield %)
1	-	KO^tBu	19
2	**1**	KO^tBu (0.1 eq)	38
3	**1**	KO^tBu (0.5 eq)	90
4	**1**	KO^tBu (0.75 eq)	92
5	**1** (2.5 mol%)	KO^tBu	61
6	**1** (7 mol%)	KO^tBu	91
7	**1** (5 mol%)	KOH	46
8	**1** (5 mol%)	K_2CO_3	0
9[a]	**1** (5 mol%)	KO^tBu	59
10[b]	**1** (5 mol%)	KO^tBu	85
11[c]	**1** (5 mol%)	KO^tBu	25
12[d]	**1** (5 mol%)	KO^tBu	43
13[e]	**1** (5 mol%)	KO^tBu	53
14[f]	**1** (5 mol%)	KO^tBu	90
15	**L**	KO^tBu	28
16	**1**	-	N.R

[a]Reaction temperature 80 °C, without O_2, [b]Reaction temperature 100 °C, without O_2, [c]inert atmostphere, [d]used O_2 saturated toluene as solvent, [e]Reaction time: 6 h, [f]Reaction time: 12 h (*Optimization has been done with the help of Amreen K. Bains).

2.3.2 Optimization of reaction conditions for 1,2 di-substituted benzimidazole synthesis*

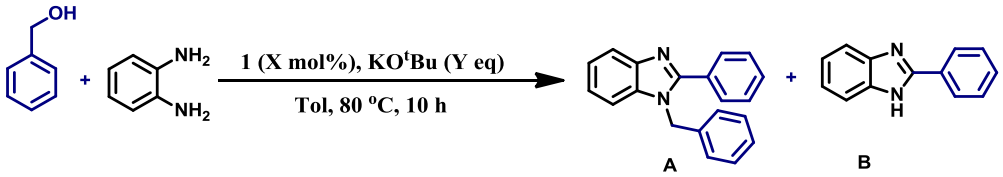

Scheme 2.3 Optimization of 1,2 di-substituted benzimidazole synthesis

Entry	Catalyst	Base	Product (Yield %), A/B
1	-	KO^{t}Bu	0/16
2	**1**	KO^{t}Bu (0.25 eq)	64/22
3	**1**	KO^{t}Bu (0.5 eq)	85/13
4	**1**	KO^{t}Bu (0.75 eq)	83/15
5	**1** (2.5 mol%)	KO^{t}Bu	61/35
6	**1** (7 mol%)	KO^{t}Bu	87/6
7	**1** (5 mol%)	KOH	25/10
8	**1** (5 mol%)	K_2CO_3	0/0
9[a]	**1** (5 mol%)	KO^{t}Bu	26/21
10[b]	**1** (5 mol%)	KO^{t}Bu	41/12
11[c]	**1** (5 mol%)	KO^{t}Bu	19/25
12[d]	**1** (5 mol%)	KO^{t}Bu	18/45
13[e]	**1** (5 mol%)	KO^{t}Bu	33/46
14[f]	**1** (5 mol%)	KO^{t}Bu	84/15
15	**L**	KO^{t}Bu	5/28
16	**1**	-	N.R

[a]Reaction temperature 80 ^{o}C, without O_2, [b]Reaction temperature 100 ^{o}C, without O_2, [c]inert atmostphere, [d]used O_2 saturated toluene as solvent, [e]Reaction time: 6 h, [f]Reaction time: 12 h (*Optimization has been done with the help of Amreen K. Bains).

2.3.3 Radical Quenching experiment

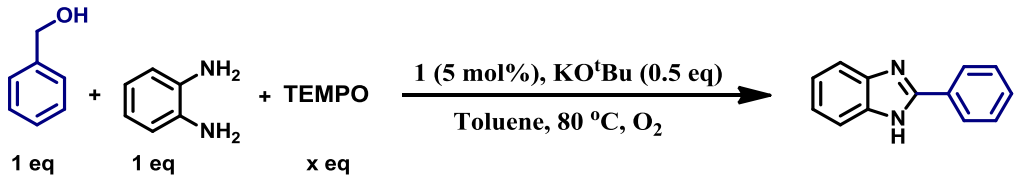

Scheme 2.4 Tempo quenching experiment

5 mL vial was charged with 1.0 mmol benzyl alcohol, 1 mmol *o*-phenylenediamine, 0.5 mmol KO^{t}Bu and 5 mol% of **1** and varying equivalent of TEMPO, followed by 2 mL toluene were added. The reaction mixture was closed with rubber septum. The resulting solution was spurged with O_2. The reaction mixture was stirred at 80 ^oC for 10 h. The product yield decreased with increasing the equivalence of TEMPO.

S.No	TEMPO equivalence	Yield (%)
1.	0.5 eq	63%
2.	1.0 eq	45%
3.	1.25 eq	38 %

Table 2.1 Tempo quenching experiment

2.3.4 Detection of H_2O_2 during alcohol oxidation

For oxidation of alcohols, presence of H_2O_2 in the reaction mixture was analyzed by UV−Vis spectroscopy using the iodometric assay based on peak of I_3^- at λ_{max} = 345 nm; ε = 26 000 M^{-1} cm^{-1} upon reaction with KI.

In a typical reaction 5 mL vial was charged with alcohols (1 mmol), KO^{t}Bu (0.25 mmol), 1 (5 mol%) in 2 mL toluene and was closed with rubber septum. The resulting solution was spurged with O_2. The reaction mixture was stirred for 2 h. After which 2 mL of water + 2 mL of DCM was added to the reaction mixture. The aqueous part was then separated. The separated aqueous layer was then acidified (to stop further oxidation) with dilute H_2SO_4 to pH = 2.

To separated aqueous layer, 1 mL of a 10% solution of KI and 2-3 drops of a 3% solution of $(NH_4)_6Mo_7O_{24}$ were added. H_2O_2 oxidizes I^- to I_2, which reacts with an excess of I^- to form I_3^-.

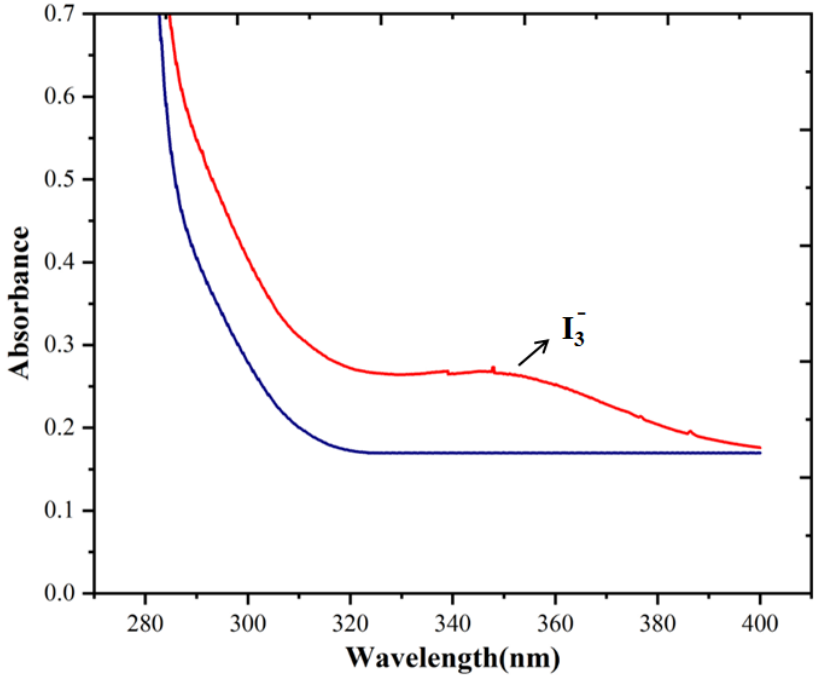

Figure 2.1 UV-Visible spectrum of (red line) I^{3-} ion formation in presence of H_2O_2, (blue line) blank.

2.3.5 Kinetic analysis for benzimidazole formation: with respect to catalyst loading

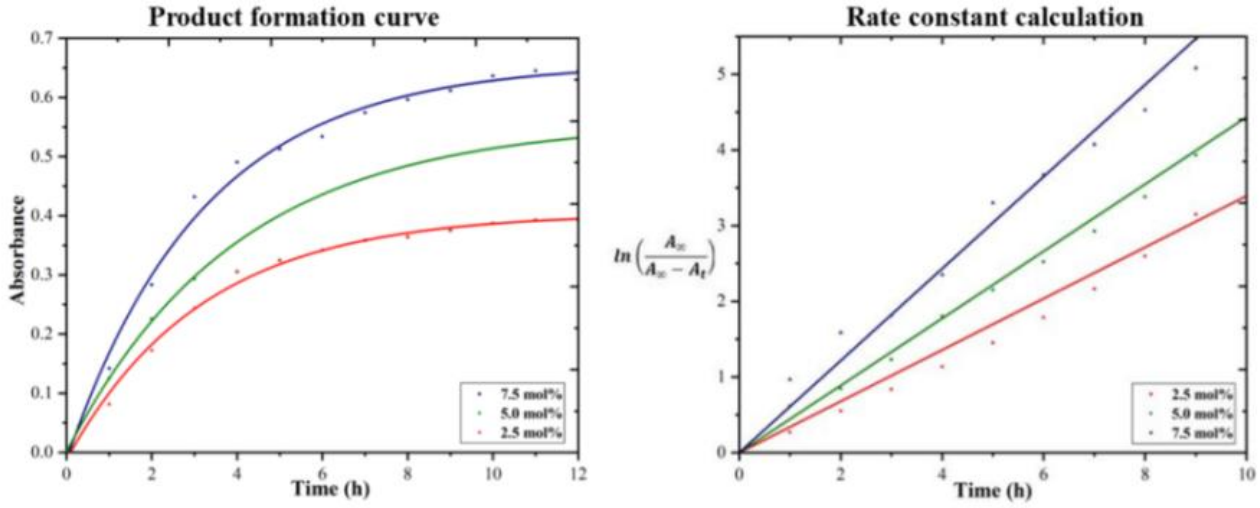

Figure 2.2 Kinetic analysis with respect to catalyst loading

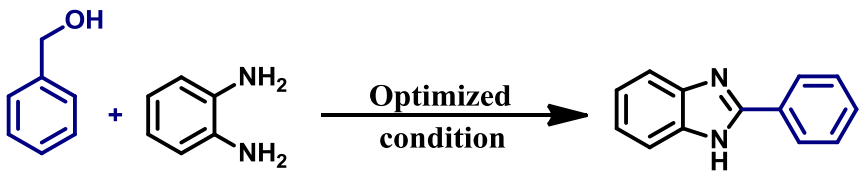

Scheme 2.5 Benzimidazole formation by varying catalyst loading

Reaction conditions: **1** (X = 2.5, 5, 7 mol%), benzyl alcohol (1 mmol), diamine (1 mmol), KO^{t}Bu (0.5 mmol), toluene (2 mL), 80 ^{o}C, O_2, 10 h.

In order to examine the dependence of reaction rate on the catalyst during benzimidazole formation, we studied the rate of benzimidazole formation as a function of catalyst loading variation. Increasing the concentration of **1** (Scheme 2.4) over the range from (x = 2.5 to 7 mol% with respect to benzyl alcohol) displayed a linear increase in the rate, k_{obs} for the oxidation of alcohol (Figure 2.2).

2.3.6 Saturation Kinetics for amine dehydrogenation

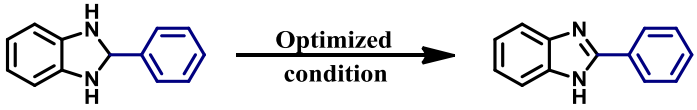

Scheme 2.6 Amine dehydrogenation

Reaction conditions: **1** (5 mol%), 3 (1 mmol), KO^{t}Bu (0.5 mmol), toluene (2 mL), 80 ^{o}C, O_2, 8 h.

Upon establishing the thorough mechanistic understanding of the first step of the reaction (Chapter 1), we have looked into the dehydrogenative aromatization step. The condensation of the aldehyde with o-phenylediamine results in imine, which upon ring cyclization yields 2,3-dihydrobenzimidazole. To examine whether the binding of 2,3-dihydrobenzimidazole is necessary during the dehydrogenation process, we performed saturation kinetics experiment with this substrate and observed a clear saturation of rate when the excess concentration of 2,3-dihydrobenzimidazole was exceeding 1.2 M (Figure 2.3 and 2.4). An equilibrium constant of 231M^{-1} and kobs of 4.5 x 10^{-4} s^{-1} was derived from the fitting of the saturation curve at 80 ^{o}C following the saturation rate law.

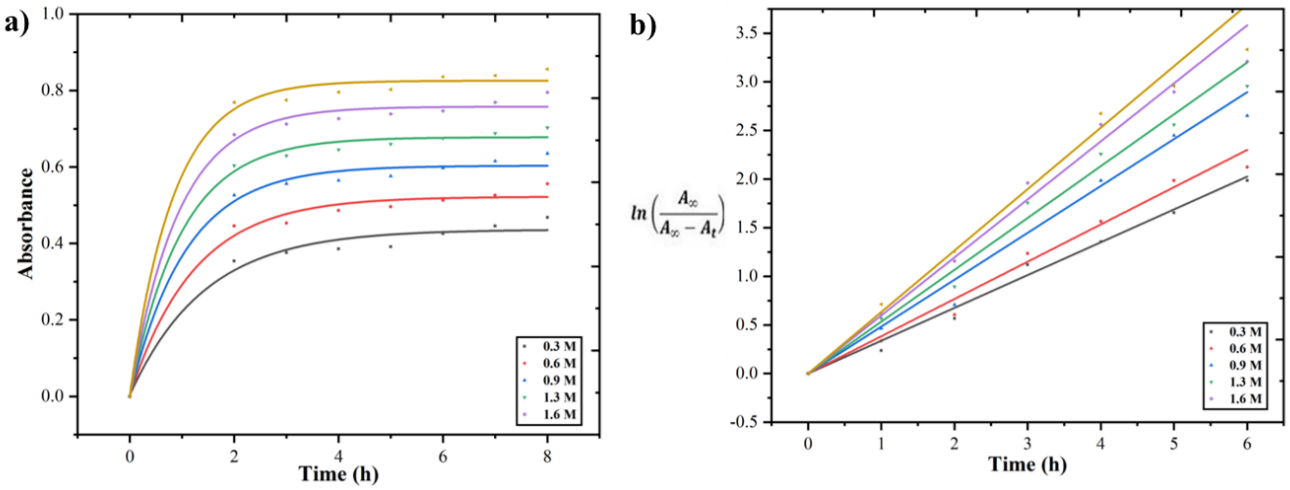

Figure 2.3 a) Kinetics profile b) Rate constant calculation for saturation kinetics profile

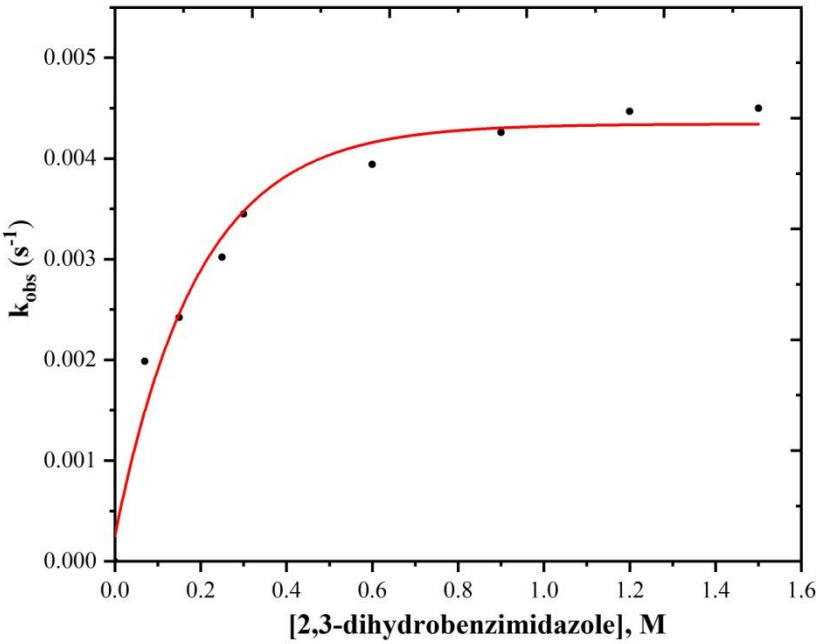

Figure 2.4 Saturation Kinetics Curve of amine dehydrogenation

2.3.7 Kinetic Isotope Effect experiment

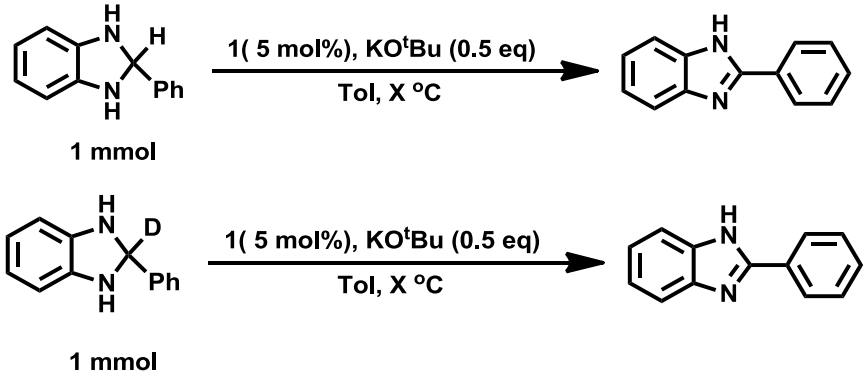

Scheme 2.7 Amine dehydrogenation by **1**

Kinetic study was performed by monitoring the reaction of 2,3-dihydro-2-phenyl-1*H*-benzimidazole and 2,3-dihydro-2-phenyl-1*D*-benzimidazole. Quantification of the amount of product and reactant was made by GC.

In a 5 mL vial, 1.0 mmol 2,3-dihydro-2-phenyl-1*H*-benzimidazole, 0.5 mmol KO^{t}Bu and 5 mol% of **1** were added followed by 2 mL toluene. The resulting solution was spurged with O_2. This reaction was heated at 60, 80 °C for 7 h (Figure 2.5).

In a 5 mL vial, 1.0 mmol 2,3-dihydro-2-phenyl-1*D*-benzimidazole, 0.5 mmol KO^{t}Bu and 5 mol% of **1** were added followed by 2 mL of toluene. The resulting solution was spurged with O_2. This reaction was heated at 60, 80 °C for 7 h (Figure 2.6).

After converting product formation curve to rate constant calculation curve (Figure 2.7) by fitting the data in first order equation, k_D was corrected using the below equation.

$$k_D(\text{corr}) = \left\{(k_D - k_H)\left(1 - \frac{DP}{100}\right)\right\}\frac{100}{DP}$$

$$DP = \text{Deuterium purity}$$

A KIE of 5.9 was measured at 60 °C. This considerably large value of KIE strongly indicates that HAT to the reduced azo backbone is rate- determining for the amine dehydrogenation reaction.

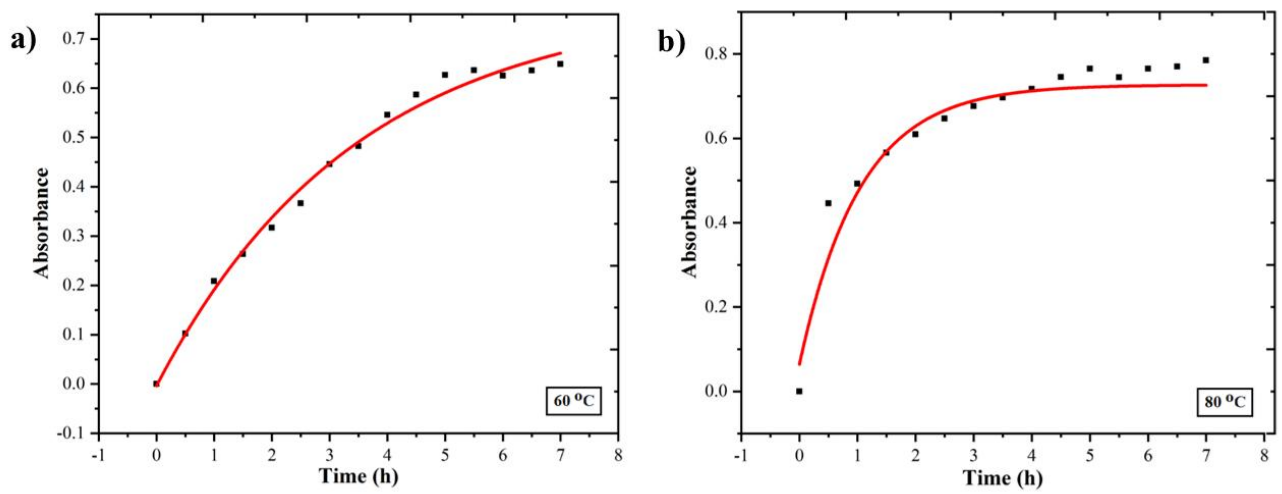

Figure 2.5 Product formation plot for 2,3-dihydro-2-phenyl-1*H*-benzimidazole at a) 60 °C,b) 80 °C.

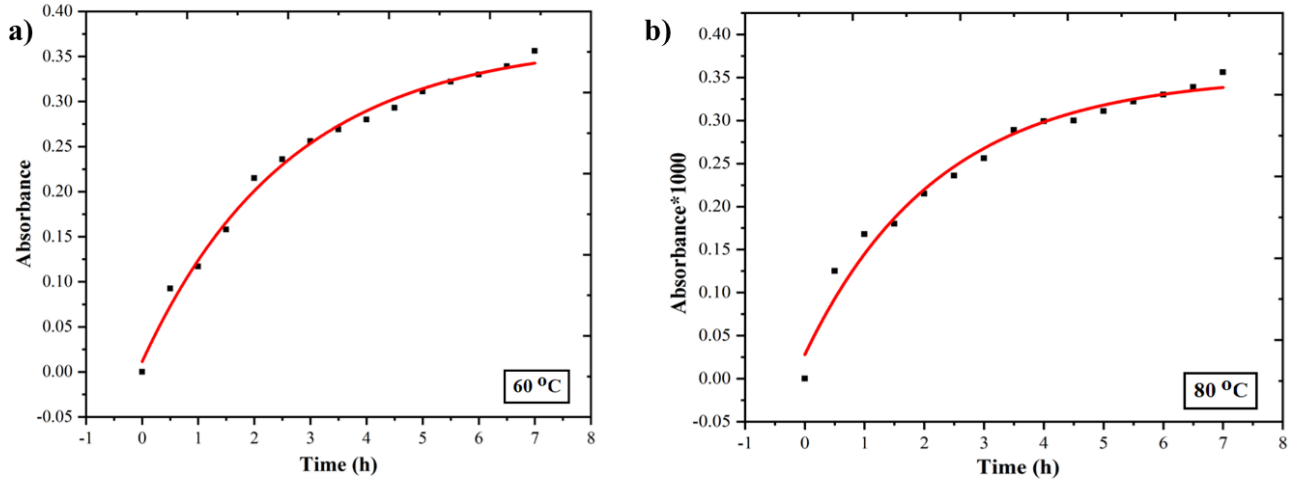

Figure 2.6 Product formation plot for 2,3-dihydro-2-phenyl-1*D*-benzimidazole at a) 60 °C, b) 80 °C.

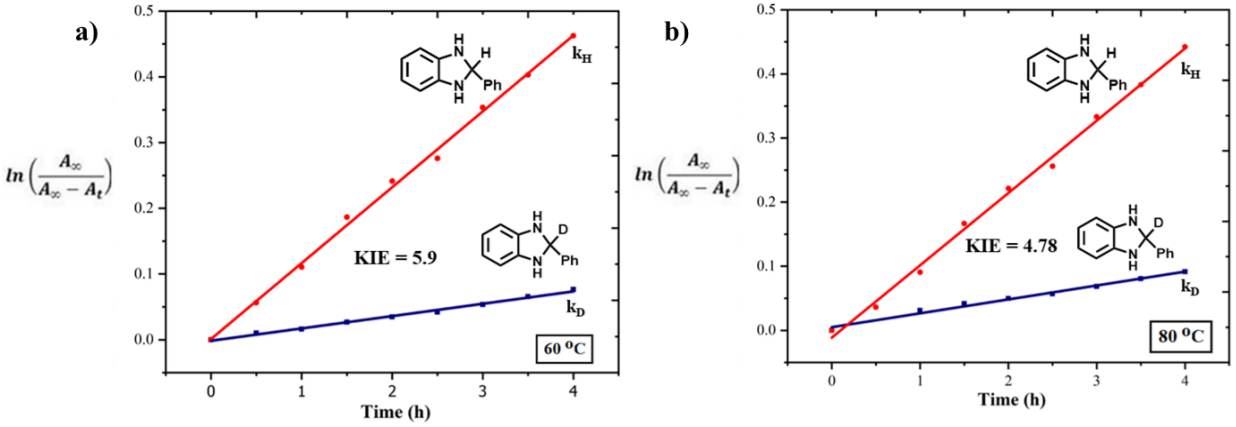

Figure 2.7 KIE for benzimidazole formation at a) 60°C, b) 80 °C.

2.3.8 Intermediate Tracking/Isolation

2.3.8.1 Intermediate - 2-amino-N-(benzylidene)aniline

In a 5 mL vial, pre-synthesized 2-amino-N-(benzylidene)aniline (1 mmol), KO^{t}Bu (0.5 mmol), **1** (5 mol%) were added followed by 2 mL toluene and was closed with rubber septum. The resulting solution was spurged with O_2. The reaction mixture was stirred at 80 ^{o}C for 5 h. Benzimidazole was isolated in 85% yield, concluding that 2-amino-N-(benzylidene)aniline is the desired intermediate in benzimidazole formation (Scheme 2.7).

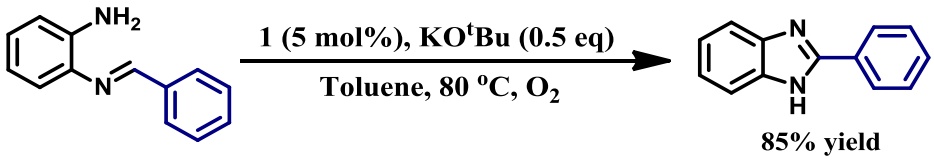

Scheme 2.8 2-amino-N-(benzylidene)aniline as an intermediate

2.3.8.2 Intermediate - 2,3-dihydro-2-phenyl-1*H*-benzimidazole

In a 5 mL vial, 2,3-dihydro-2-phenyl-1*H*-benzimidazole (1 mmol), KO^{t}Bu (0.5 mmol), **1** (5 mol%) were added followed by 2 mL toluene and was closed with rubber septum. The resulting solution was spurged with O_2. The reaction mixture was stirred at 80 ^{o}C for 10 h. Benzimidazole was isolated in 76% yield, concluding that 2,3-dihydro-2-phenyl-1*H*-benzimidazole is the required intermediate in benzimidazole formation via dehydrogenative aromatization (Scheme 2.8).

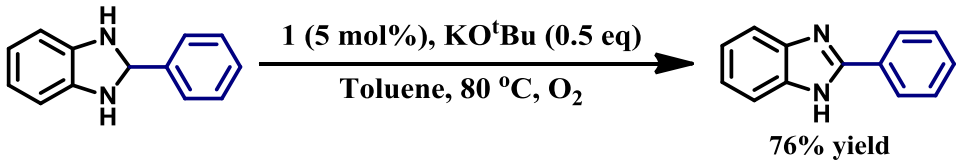

Scheme 2.9 2,3-dihydro-2-phenyl-1H-benzimidazole as an intermediate

2.3.8.3 Intermediate - *N,N*-bis(benzylidene)-1,2-diaminobenzene

In a 5 mL vial, benzyl alcohol (2 mmol), *o*-phenylenediamine (1 mmol), KO^{t}Bu (0.5 mmol), **1** (5 mol%) were added followed by 2 mL toluene and was closed with rubber septum. The resulting solution was spurged with O_2. The reaction mixture was stirred at 80 ^oC for 5 h. 1,2 di-substituted benzimidazole was obtained along with *N,N*-bis(benzylidene)-1,2-diaminobenzene. This experiment concludes that *N,N*-bis(benzylidene)-1,2-diaminobenzene is the desired intermediate towards 1,2 di-substituted benzimidazole formation. The targeted intermediate was characterised by ESI-MS. ($M+H^+$ = 285.1386) (Scheme 2.8)

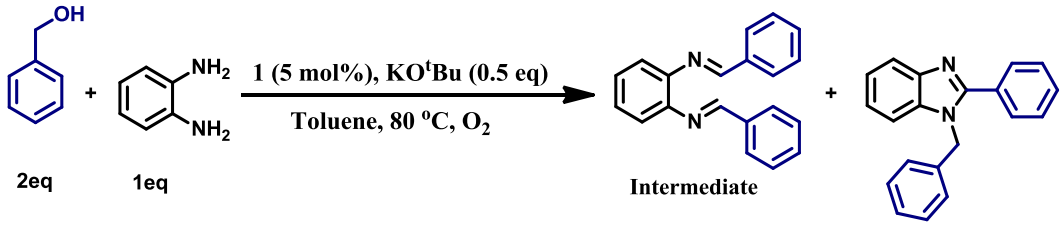

Scheme 2.10 N,N-bis(benzylidene)-1,2-diaminobenzene as an intermediate.

2.3.9 N-alkylation of Benzimidazole

In a 5 mL vial, benzyl alcohol (1 mmol), benzimidazole (1 mmol), KO^{t}Bu (0.5 mmol), **1** (5 mol%) were added followed by 2 mL toluene and was closed with rubber septum. The resulting solution was spurged with O_2. The reaction mixture was stirred at 80 ^oC for 10 h. 1,2 di-substituted benzimidazole was not obtained indicating N-alkylation of benzimidazole pathway is excluded for 1,2 di-substituted benzimidazole formation (Scheme 2.9).

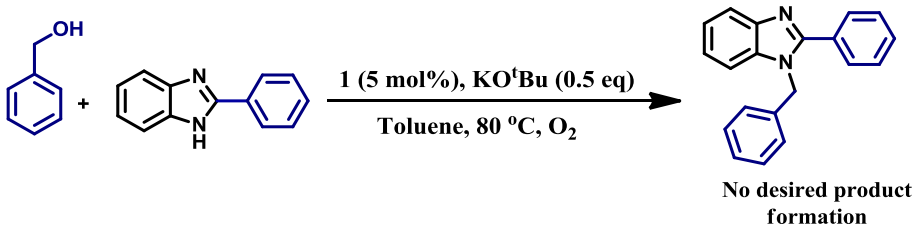

Scheme 2.11 N-alkylation of Benzimidazole

2.4 Summary

In this chapter, we mainly discussed synthesis of benzazoles and established a thorough mechanistic understanding. We synthesized a wide array of benzimidazoles, using **1** by simply controlling the stoichiometry of benzyl alcohol. Along this direction, we changed the *o*-phenylene diamine with *o*-amino phenol and *o*-amino thiol. The corresponding benzoxazoles and benzthiazoles were synthesized in good to excellent yields.

The two-electron oxidation of alcohols, and oxidative dehydrogenation of 2,3-dihydrobenzimidazole is greatly facilitated by azo-hydrazo redox couple, which is an integral component of the ligand backbone. Moreover, the hydrazo moiety can be reoxidized to the catalytically relevant azo form via simply oxidizing by oxygen gas. Both alcohol oxidation and dehydrogenative aromatization of 2,3-dihydrobenzimidazole are exclusively mediated by a rate-limiting HAT steps.

We have done an ample amount of experiments to rigorously prove the presence of HAT. Starting from the saturation kinetics experiment to establish the binding of 2,3-dihydrobenzimidazole during the dehydrogenation step, KIE determination to prove HAT as rate determining step and isolating all the intermediates. The presence of H_2O_2 is detected using iodometric titrations during the course of the reaction.

Bibliography

1. Zweig J.E., Kim D.E., Newhouse T.R. Methods Utilizing First-Row Transition Metals in Natural Product Total Synthesis. *Chem. Rev.* **2017**, *117*, 11680–11752.
2. Luca, Oana R., and Robert H. Crabtree. Redox-active ligand in catalysis. *Chemical Society Reviews*, **2013**.
3. Chong C.C., Kinjo R. Catalytic Hydroboration of Carbonyl Derivatives, Imines, and Carbon Dioxide. *ACS Catal*. **2015**, *5*, 3238–3259.
4. Díez-González S., Nolan S.P. Transition Metal-Catalyzed Hydrosilylation of Carbonyl Compounds and Imines. A Review. Org. Prep. Proced. Int. **2007**, *39*, 523–559.
5. Alberico D., Scott M.E., Lautens M. Aryl-Aryl Bond Formation by Transition Metal Catalyzed Direct Arylation. *Chem. Rev.* **2007**, *107*, 174–238.
6. Jiao J., Murakami K., Itami K. Catlytic Methods for Aromatic C-H Amination: An Ideal Strategy for Nitrogen-based Functional Molecules. *ACS Catal.* **2016**, *6*, 610–633.
7. Albrecht M., Bedford R., Plietker B. Catalytic and Organometallic Chemistry of Earth-Abundant Metals. *Organometallics.* **2014**, *33*, 5619–5621
8. Campeau L.-C., Hazari N. Cross-Coupling and Related Reactions: Connecting Past Success to the Development of New Reactions for the Future. *Organometallics.* **2019**, *38*, 3–35
9. C. K. Jørgensen. *Coord. Chem. Rev*., **1966**, *1*, 164.
10. W. I. Dzik, J. I. van der Vlugt, J. N. H. Reek and B. de Bruin. Ligands that store and release electrons during catalysis. *Angew. Chem., Int. Ed.,* **2011**, *50*, 3356.

11. S. Das, C. D. Incarvito, R. H. Crabtree and G. W. Brudvig. Molecular recognition in the selective oxygenation of saturated CH bonds by a dimanagaese catalyst. *Science*, **2006**, *312*, 1941.
12. S.Das, G.W. Brudwig and R.H. Crabtree, Molecular recognition in homogenous transition metal catalysts : a biometric strategy for high selectivity. *Chem. Commun*., **2008**, *413*.
13. James M. Mayer. Understanding Hydrogen Atom Transfer: From Bond Strengths to Marcus Theory. *Accounts of Chemical Research*, **2011.**
14. Huynh, M. H. V.; Meyer, T. J. Proton-Coupled Electron Transfer. *Chem. Rev.* **2007**, *107*, 5004–5064.
15. Bains, A. K.; Kundu, A.; Yadav, S.; Adhikari, D., Borrowing Hydrogen-Mediated N-Alkylation Reactions by a Well-Defined Homogeneous Nickel Catalyst. *ACS Catal.* **2019,** *9*, 9051-9059.
16. Wijeratne, G. B.; Corzine, B.; Day, V. W.; Jackson, T. A., Saturation Kinetics in Phenolic O–H Bond Oxidation by a Mononuclear Mn(III)–OH Complex Derived from Dioxygen. *Inorg. Chem*. **2014**, *53*, 7622-7634.
17. Gardner, K. A.; Kuehnert, L. L.; Mayer, J. M., Hydrogen Atom Abstraction by Permanganate:? Oxidations of Arylalkanes in Organic Solvents. *Inorg. Chem.* **1997**, *36*, 2069-2078.
18. Wang, Y.; DuBois, J. L.; Hedman, B.; Hodgson, K. O.; Stack, T. D. P., Catalytic Galactose Oxidase Models: Biomimetic Cu(II)-Phenoxyl-Radical Reactivity. *Science* **1998**, *279*, 537-540.
19. Reed-Berendt, B. G.; Polidano, K.; Morrill, L. C., Recent Advances in Homogeneous Borrowing Hydrogen Catalysis using Earth-Abundant First Row Transition Metals. *Org. Biomol. Chem*. **2019**, *17*, 1595-1607.

20. Hille, T.; Irrgang, T.; Kempe, R., The Synthesis of Benzimidazoles and Quinoxalines from Aromatic Diamines and Alcohols by Iridium-Catalyzed Acceptorless Dehydrogenative Alkylation. *Chem. Eur. J.* **2014,** *20*, 5569-5572.
21. Watanabe, Y.; Tsuji, Y.; Ohsugi, Y. The Ruthenium Catalyzed N-Alkylation and N-Heterocyclization of Aniline using Alcohols and Aldehydes. *Tet. Lett.* **1981**, *22*, 2667 - 2670.
22. Tateyama, K.; Wada, K.; Miura, H.; Hosokawa, S.; Abe, R.; Inoue, M.. Dehydrogenative Synthesis of Benzimidazoles under Mild Conditions with Supported Iridium Catalysts. *Catal. Sci. Tech.* **2016**.
23. Daw, P.; Ben-David, Y.; Milstein, D. Direct Synthesis of Benzimidazoles by Dehydrogenative Coupling of Aromatic Diamines and Alcohols Catalyzed by Cobalt. *ACS Catal.* **2017**, *7*, 7456-7460.